Fatigue damage in copper polycrystals subjected to ultrahigh-cycle fatigue below the PSB threshold

Anja Weidner[1,a], Dorothea Amberger[2,b], Florian Pyczak[2,c], Bernd Schönbauer[3,d], Stefanie Stanzl-Tschegg[3,e] and Hael Mughrabi[3,f]

[1]Technische Universität Dresden, Institut für Strukturphysik, 01062 Dresden, Germany

[2,3,6]Universität Erlangen-Nürnberg, Department of Materials Science and Engineering, General Materials Properties, Martensstr. 5, 91058 Erlangen, Germany

[4,5] Universität für Bodenkultur, Department für Materialwissenschaften und Prozesstechnik, Peter Jordanstr. 82, 1190 Vienna, Austria

[a]aweidner@physik.tu-dresden.de, [b]dorothea.amberger@ww.uni-erlangen.de, [c]florian.pyczak@ww.uni-erlangen.de, [d]bernd.schoenbauer@boku.ac.at, [e]stefanie.tschegg@boku.ac.at, [f]mughrabi@ww.uni-erlangen.de

Keywords: UltraHigh Cycle Fatigue, Very High Cycle Fatigue, copper, PSB threshold, dislocation microstructure, cyclic strain localization, fragmentation of grain boundaries, surface roughness, stage I microcracks, fatigue damage

Introduction

There is currently an increased interest in understanding the specific damage and failure mechanisms which occur in the UltraHigh-Cycle Fatigue (UHCF) or Very High Cycle Fatigue (VHCF) range above about 10^8 to 10^9 cycles. Most current studies have focused on the UHCF behaviour of high-strength materials containing microstructural heterogeneities, in which internal fatigue failure frequently is caused by fatigue cracks which are initiated at internal heterogeneities such as inclusions, compare [1]. In contrast, the present work is part of an experimental study of the UHCF behaviour of pure ductile single-phase face-centred cubic (fcc) materials such as copper. In these materials, the most common high-cycle fatigue (HCF) failure modes originate from cyclic strain localization in persistent slip bands (PSBs). The general belief is that a necessary prerequisite for cyclic strain localization in PSBs is that the so-called PSB threshold amplitude [2] must be exceeded. However, it had been postulated in earlier work that, even at very low amplitudes, cyclic slip still retains a small but non-negligible irreversible component which, accumulated in a random fashion over a very large number of cycles in the UHCF regime, can lead to surface roughening (and irreversible changes of the dislocation substructure) and, ultimately, perhaps to PSB formation and fatigue crack initiation. In that picture, fatigue damage can be expected to develop in the UHCF regime even below the PSB threshold [3], as illustrated in Fig. 1 (σ: stress, axis vertical).

In order to test this hypothesis, a project was started in which the UHCF behaviour of commercial purity copper polycrystals that had been ultrasonically fatigued up to more than 10^{10} cycles was investigated in some detail. In this work, a detailed study of the surface features was conducted by scanning electron microscopy (SEM) and atomic force microscopy (AFM). The most important results of this earlier work have been published [4,5,6] and are summarized as follows:

- The "traditional" axial PSB threshold stress amplitude was found to be ca. 63 MPa [4,5,6].
- Well below the PSB threshold, marked cyclic slip localization occurred in intense slip bands after very large numbers of cycles and intensified with increasing numbers of cycles [4,5].

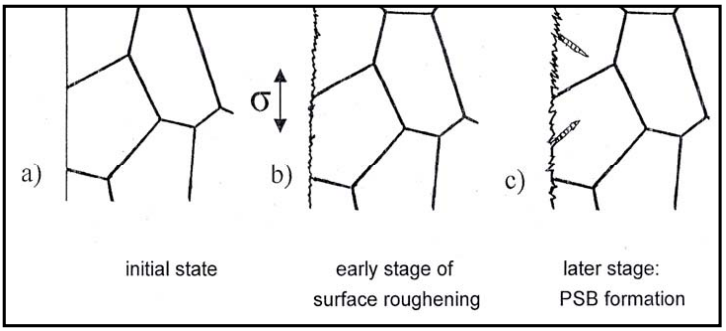

Fig. 1: Schematic illustration of b) surface roughening and c) PSB formation. After [3].

- The slip bands were shown to be persistent [6] in the sense that, when the surface was electropolished after fatigue, they reappeared at the same sites on the surface when fatigue was resumed. Hence, in analogy to [7], they are considered "persistent" slip bands (PSBs).
- At the sites of emerging PSBs at the surface, extrusions and intrusion-like deepenings (microcracks) formed [4,5,6].
- The observations showed clearly that the magnitude of the PSB threshold (and the fatigue limit) is not constant but depends on the number of cycles, being the lower the higher the number of cycles [4,5,6], in accord with the predictions of the model described above [3].

The present work focuses on the microstructural analysis of the fatigue-induced features and damage at the surface and in the bulk, as studied with SEM and the focused ion beam (FIB) technique. The dislocation microstructures were analyzed in surface grains and in interior grains by the electron channeling contrast (ECC) technique in the SEM [8]. These studies provided convincing evidence that *different kinds of fatigue damage occurred in the UHCF regime below the PSB threshold*. In the following, these recent observations will be presented and discussed.

Experimental

A polycrystalline rod of commercial purity copper (mean grain size: ca. 60 μm) of 7 mm diameter and 80 mm in length was fatigued ultrasonically at a frequency of 19 kHz with pulse-pause sequences, as described in more detail previously [4,5,6]. The axial stress amplitude at the location of highest stress was ca. 61.5 MPa. Fatigue loading was interrupted repeatedly in order to perform surface studies by scanning electron microscopy (SEM) and atomic force microscopy (AFM) after different numbers of cycles [4,5]. All studies reported here were performed on that specimen after it had been fatigued for a total of 1.59×10^{10} cycles. For the following, it is important to note that the distribution of the axial stress amplitude along the specimen was sinusoidal with the site of maximum stress amplitude located at a distance of 48 mm from the free end and 32 mm from the clamped end of the rod. Hence, by studying different sections of the specimen at defined distances from the position of maximum stress, it was possible to investigate on one and the same specimen locations that had experienced different stress amplitudes (ranging from 0 to 61.5 MPa).

The studies with the FIB technique were performed on a Zeiss CrossBeam 1540 ESB instrument. In these studies, the following procedure was adopted. Almost all surface grains of the fatigued rod specimen were covered more or less densely with the traces of a large number of "PSBs". For the FIB studies, grains were selected in which the slip band traces lay roughly perpendicular to the direction of the rod (stress) axis. In that case, it could be assumed that the plane of the PSBs would lie approximately under 45º to the direction of the stress axis and that the active Burgers vector would lie roughly in the plane perpendicular to the PSB traces (and in the PSB planes). Next, a thin

platinum layer was deposited on a small area covering the PSB traces. Then, the FIB micro-machining technique was used to cut by ion sputtering a plane perpendicular to the PSB traces through the platinum layer into the copper material. This plane was then studied in the electron scanning mode. The surface topography of the fatigued specimen was clearly recognizable as a sharp line delineating the interface between the platinum layer and the copper. Then the whole rod was electrocoated with a 0.5 mm thick copper layer to protect the surface and was then cut parallel to the axis into two halves. After chemical and electrolytic polishing of the cut plane, the dislocation microstructures were studied by ECC/SEM at different sites near and further away from the surface in a Zeiss Ultra55 FESEM (field emission scanning electron microscope), equipped with an In-lens-SE-detector (SE: secondary electron) and an angular selective 4-quadrant backscatter electron (BSE) detector. The surface was easily recognizable as the borderline between the specimen and the electrocoating. Some pictures were also made on the SEM of the FIB instrument.

Observations and Discussion

FIB observations of surface roughness and stage I (shear) cracks. Figures 2 and 3 show examples of SEM micrographs obtained on the ion-machined surface that was approximately perpendicular to the surface traces of the PSBs. Fig. 2 was taken at a surface site at a distance from the location of maximum stress where the local stress amplitude had been ca. 57 MPa, i.e. about 6 MPa below the "traditional" PSB threshold stress amplitude of ca. 63 MPa, which had been determined after 10^6 cycles in ultrasonic fatigue tests [4,5,6], thus being higher than the PSB threshold stress of ca. 56 MPa at conventional frequencies [9]. In Fig. 2, the original PSB surface markings and the deposited platinum layer are clearly visible. In addition, the following features are noteworthy. At the interface between the platinum coating and the copper specimen, there is a marked surface roughness profile which is more clearly recognizable at higher magnifications. Then there is a family of roughly parallel cracks, aligned under an angle of about 45° to the stress axis. These cracks are regarded as mode II stage I shear cracks. Fig. 3 was taken at higher magnification at the location of maximum stress amplitude (61.5 MPa), i.e. ca. 1.5 MPa below the PSB threshold. Here, the surface roughness can be recognized clearly in addition to the stage I shear cracks. It can be seen that some cracks have been initiated at stress raisers in the surface roughness. The latter lends itself to a semi-quantitative evaluation as described below. If it is assumed that the roughness profile has been generated by random slip, it can be characterized by the root mean square displace-

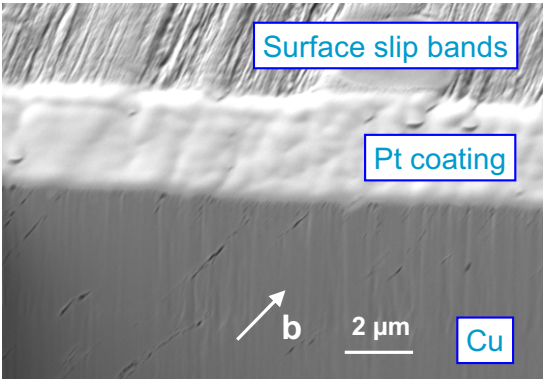

Fig. 2: FIB micrograph, showing original surface slip bands, platinum coating and micro-machined plane roughly perpendicular to the plane of the slip bands with fatigue-induced surface roughness visible at the copper specimen-platinum coating interface. Note family of stage I shear cracks. About 6 MPa below PSB threshold. Specimen axis horizontal.

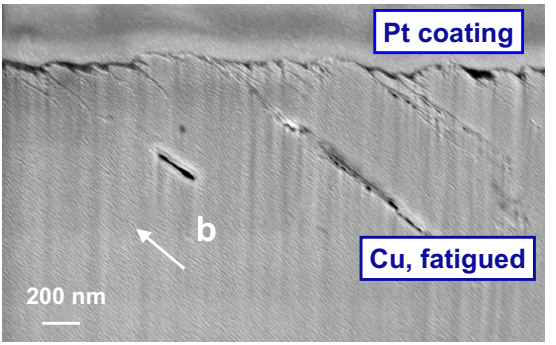

Fig. 3: FIB micrograph showing surface roughness at interface between platinum layer and fatigued copper specimen and stage I microracks. About 1.5 MPa below PSB threshold. Specimen axis horizontal.

ment (rms), measured parallel to the Burgers vector **b** [3]:

$$\sqrt{< x^2 >} = K\sqrt{4N\gamma_{pl,loc}\, p\, b\, h} = (\text{rms}) \qquad (1)$$

Here, N is the number of cycles, $\gamma_{pl,loc}$ is the local shear strain amplitude, b is the modulus of the Burgers vector and p is the so-called irreversibility of slip which is defined as the fraction of cyclic slip ($0 < p < 1$) that is irreversible [2, 3]. The quantity h has two possible meanings. When one considers the root mean square displacement between neighbouring atomic slip planes, then h is the glide plane spacing and the constant K in the equation is equal to 1. When one refers, however, to the peak-to-valley roughness, then h is the length along which the peak-to-valley roughness is measured, and the constant K is approximately equal to 1.2 [10]. In the present context, this latter case is of interest. From Fig. 3, a peak-to-valley roughness of ca. 150 nm, measured parallel to **b** ($b = 2.5\times10^{-10}$ m) over a distance $h \approx 2$ µm, can be evaluated. The local plastic shear strain amplitude can be written as $\gamma_{pl,loc} = M\times\Delta\varepsilon_{pl,loc}/2$, where M is an orientation factor (taken as the Sachs factor = 2.24) and $\Delta\varepsilon_{pl,loc}/2$ the local axial plastic strain amplitude. The value of $\Delta\varepsilon_{pl,loc}/2$ is taken to be 6.1×10^{-6} which corresponds to the PSB threshold value of the axial plastic strain amplitude, as measured at ultrasonic frequency [5,6]. Then, one can obtain from Eq. 1 an estimate for the cyclic slip irreversibility p which is the only unknown quantity in Eq. 1 and which is not well known and generally difficult to assess. Inserting all quantities, one obtains $p \approx 0.000036$ which is very small, as expected. However, for the present very large number of cycles N in the UHCF regime (i.e. $N = 1.59\times10^{10}$ cycles), this small irreversibility gives rise to a substantial cumulative irreversible plastic shear strain $4N\cdot\gamma_{pl,loc}\cdot p \approx 31$!! The microstructural origin of cyclic slip irreversibility and the implications in the present case will be discussed in a later section.

ECC/SEM observations of dislocation patterns and fatigue damage. Figs. 4a and 4b are examples of the ECC/SEM imaging of a surface site at a distance from the location of maximum axial stress amplitude (local stress amplitude ca. 54 MPa, i.e. about 9 MPa below PSB threshold). Fig. 4b, taken with the In-Lens-SE detector, shows particularly clearly the original specimen surface as the interface between the electrocoating (at the top) and the specimen, showing a marked surface roughening and, in addition, several sites of stage I crack initiation in the valleys of the roughness profile. These findings confirm the FIB observations and substantiate the conclusion that surface roughening and stage I crack initiation occurred at stress amplitudes well below the PSB threshold. Fig. 4a, taken with the BSE detector, does not show these details but provides complementary information concerning the dislocation microstructure, revealing that cyclic slip occurred in a localized fashion in slip lamellae aligned close to 45º with respect to the stress axis.

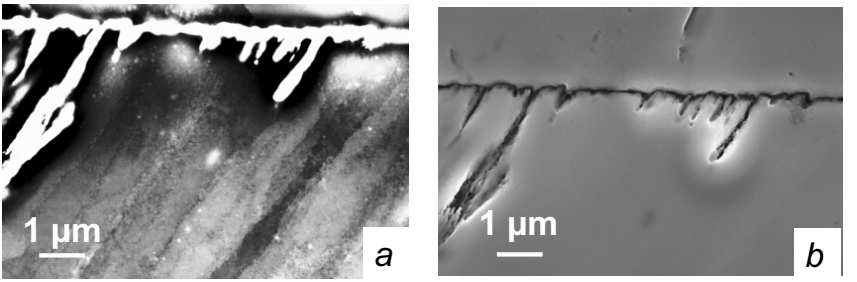

Fig. 4: Fatigue-induced surface roughness and stage I crack initiation from a location where the local stress amplitude was about 57 MPa, i.e. ca. 6 MPa below the PSB threshold. a) backscattered electron SEM/ECC image. b) same area, taken with In-Lens-SE detector. Specimen axis horizontal.

Similar dislocation patterns, indicative of localized deformation in slip lamellae, aligned very roughly under an angle of 45º to the stress axis, were also observed in interior grains, as shown in Fig. 5, both at the location of maximum stress (Fig. 5a) and also in areas of significantly smaller stress amplitude (Fig. 5b). Fig. 6a shows another example of such localized slip lamellae in an area of even lower local stress amplitude (ca. 48 MPa, i.e. ca. 15 MPa below the PSB threshold). The dislocation microstructure in the slip lamellae observed was mainly an elongated cell structure. Sometimes slip lamellae with ladder-like dislocation patterns, looking like remnants of PSBs with the classical ladder structure, next to vein-like dislocation patches, were also found in such areas of lower stress amplitude. Fig. 6b shows an example (ca. 54 MPa, i.e. ca. 9 MPa below the PSB threshold). In regions of lower stress amplitude levels such as in Fig. 6a, the surface roughening was much less pronounced than in areas of higher stress amplitude. Figure 7 shows an example of a surprising observation in an interior grain at the location of maximum stress amplitude, showing clearly what looks like a family of microcracks, some microns long, lying roughly under an angle of 45º to the stress axis, looking very much like "interior" stage I shear microcracks. Similar "microcracks" were also found in interior grains in areas of much lower stress amplitude but much less frequently.

Finally, Fig. 8 shows another surprising observation made in interior grains. Quite commonly, the grain boundaries were heavily fragmented, indicative of grain boundary displacements up to about one micron. On the one hand, the displacements look irregular. On the other hand, they do seem to be spatially correlated to the slip lamellae.

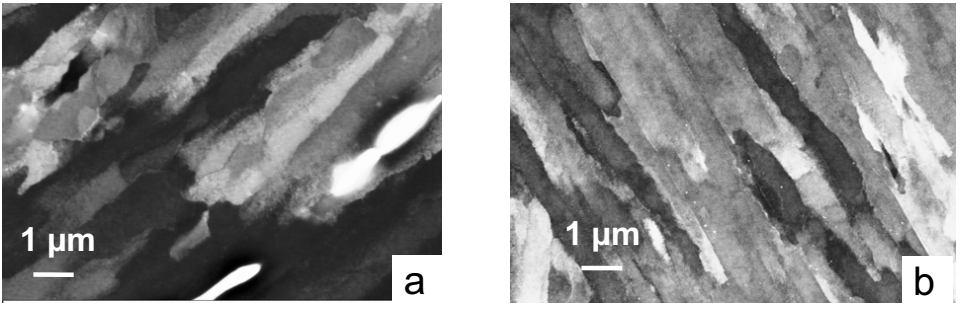

Fig. 5: ECC/SEM images of localized cyclic slip lamellae in interior grains. a) at the location of maximum stress amplitude (61.5 MPa, i.e. ca. 1.5 MPa below PSB threshold). b) away from the location of maximum stress amplitude (local stress amplitude about 54 MPa, i.e. ca. 9 MPa below PSB threshold). Specimen axis horizontal.

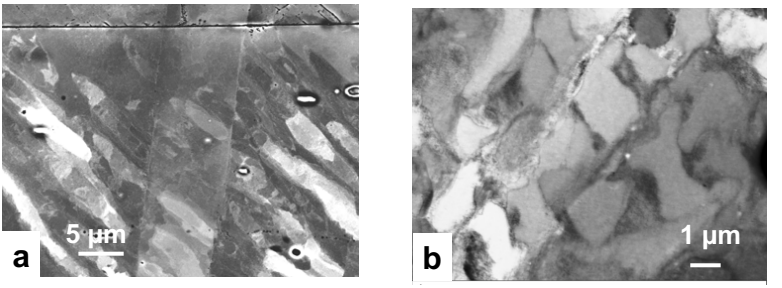

Fig. 6: ECC/SEM: Regions of localized deformation in slip lamellae. a) surface grain, ca. 15 MPa below PSB threshold. b) Interior grain, with ladder-like slip lamella, ca. 9 MPa below PSB threshold. Stress axis horizontal.

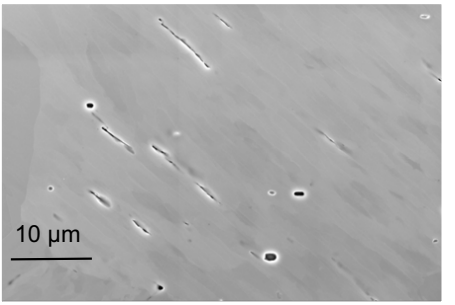

Fig. 7: Stage I "microcracks" in interior grain, region of maximum stress amplitude (ca. 61.5 MPa, i.e. ca. 1.5 MPa below PSB threshold). ECC/SEM (In-Lens-SE detector). Stress axis horizontal.

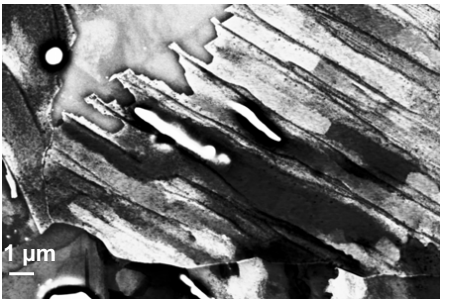

Fig. 8: ECC/SEM image of fragmented grain boundary in interior grain in region of maximum stress amplitude (61.5 MPa, i.e. ca. 1.5 MPa below PSB threshold). Stress axis horizontal.

Concluding Discussion of Main Features

Evolution of dislocation microstructure and fatigue damage. In agreement with the earlier results[4,5,6], it is now clear that, after a sufficiently large number of cycles in the UHCF range, *fatigue damage develops at loading amplitudes below the traditional PSB threshold amplitudes*. The damage occurs in the form of cyclic strain localization, surface roughening and stage I shear "microcrack" initiation at the surface and in the bulk. The dislocation patterns observed differ from the matrix structure of veins and PSBs with the ladder structure found at conventional frequencies (and numbers of cycles) in cyclic saturation in HCF. The fragmentation of the grain boundaries is a phenomenon that has not been encountered before. In the following, some details will be discussed.

Lamellae of localized shear deformation. These lamellae are reminiscent of "old" PSBs in which the ladder structure has been transformed into a cell structure due to the accumulated effect of slip irreversibilities and slowly increasing secondary slip, as shown earlier for copper single crystals that acquired a very long life during fatigue in vacuum [11]. This shows clearly that, even in so-called cyclic "saturation", the small fraction of slip that is irreversible, which is caused, for example, by mutual dislocation annihilations [2], leads to a slow persistent modification of the dislocation distribution. In the present case, it is proposed that a classical vein matrix structure probably forms first but then continues to harden very slowly so that some form of PSBs would develop *even below the PSB threshold*. The fact that in regions of lower local stress amplitude remnants of a wall structure were sometimes seen suggests that at an earlier stage the originally formed PSBs may have had the ladder structure. These PSBs would then also harden very slowly and would eventually be replaced by new ones which would suffer the same fate, etc. [11]. In this manner, provided that cyclic deformation is performed to very large numbers of cycles, most of the grains that are favourably orientated (for slip on a "dominant" glide plane) would gradually become filled with the lamellae of localized slip observed in this study. It is assumed that, because of the different ages and prehistories of these lamellae, they would differ in their glide activities.

Evolution of surface roughness, cyclic strain localization and crack initiation. Eq. 1 is based on the assumption that surface roughness develops as a result of the irreversible component of random slip [3]. This is only approximately true before severe strain localization sets in. Hence, the roughness seen could be partially due to random slip and to the other part a result of localized slip with extrusion formation, etc. Crack initiation at the surface could be promoted by either form of roughness. However, it is important to note that lamellae of cyclic strain localization were observed not only in surface but also in interior grains. Hence, cyclic strain localization can be expected to develop in surface (and in other) grains even in the absence of the surface roughening proposed in the model [3] and would by itself lead to extrusions, etc., and contribute to fatigue crack initiation.

Stage I shear microcracks. It is difficult to imagine that the "microcracks" that have been seen and that lay without exception roughly under 45º to the stress axis are anything else but stage I shear cracks. This assumption applies not only to those cracks that originated from stress raisers in the roughness profile but also to the "interior" stage I cracks, although it is not readily understood how such cracks could form inside bulk grains. It may have played a role that the copper investigated was of commercial purity. During cyclic deformation point defects, in particular vacancies, are formed continuously. These vacancies can migrate at room temperature. Hence, it is conceivable that in regions of high glide activity foreign atoms can diffuse and segregate to "potential crack sites" and promote "interior" crack initiation. To verify this hypothesis, more rigorous examination is necessary, for example by checking whether interior cracks form also in high-purity material.

Local displacements and fragmentation of grain boundaries. It has been observed that, at higher temperatures, grain boundaries undergo discrete displacements during each cycle of deformation [12,13,14]. The magnitude of these displacements depends on the character of the grain boundaries. The displacements are thermally activated and have been suggested to be driven by the driving force for grain coarsening [13,14]. In the present case, one can hardly speak of high temperature fatigue. Nonetheless, vacancies are produced and can migrate. They can hence assist very small thermally activated displacements of the grain boundaries per cycle which, accumulated over the very large numbers of cycles to which the specimen has been exposed, could lead to measurable displacements. In the present case, the main driving force for the irregular grain boundary displacements which are correlated spatially with the locations of the slip lamellae is suggested to lie in the unequal dislocation fluxes on either side of the grain boundaries, caused by different orientation factors of the grains and different forms of slip localization within the grains.

Summary

The present work, in combination with the earlier studies on the UHCF behaviour of polycrystalline copper [4,5,6], confirms that, provided the number of cycles is large enough, *substantial fatigue damage does develop at loading amplitudes well below the PSB threshold* in the form of

- cyclic slip localization in shear lamellae [4,5,6] containing elongated dislocation cells,
- a pronounced fatigue-induced surface roughening [4,5], and
- initiation of stage I (mode II) shear cracks which, interestingly enough, were found not only at the surface but also in interior grains.
- The severity of all features of fatigue damage decreased with increasing distance from the surface and with decreasing local stress amplitude.

In addition, substantial local grain boundary displacements were noted. The fatigue damage observed is more complex than predicted by the earlier model [3]. Since the fatigue limit lies above the PSB threshold [9], it remains an open question whether the fatigue damage observed can finally lead to fatigue failure. The newly found microstructural features should be studied further as a function of numbers of cycles *N*, and the results should be implemented in a more refined model.

References

[1] Proceedings of Fourth International Conference on Very High Cycle Fatigue (VHCF-4), edited by J. E. Allison et al., TMS (2007).

[2] H. Mughrabi, F. Ackermann and K. Herz, in: Fatigue Mechanisms, ASTM STP 675, edited by J.T. Fong, American Society for Testing and Materials, Philadelphia (1979), p. 731.

[3] H. Mughrabi, Int. J. Fatigue 28 (2006) 1501.

[4] S. Stanzl-Tschegg, H. Mughrabi H. and R. Schuller in: Fracture of Nano- and Engineering Materials and Structures, Proceedings of 16th European Conference ofFracture (ECF 16), no. 458. edited by E.E. Gdoutos, Springer, 2006, ISBN-10 1-4020-4971-4.

[5] S. Stanzl-Tschegg, H. Mughrabi and B. Schoenbauer, Int. J. Fatigue 29 (2007) 2050.

[6] S. Stanzl-Tschegg, B. Schoenbauer and C. Laird, in: Plasticity, Failure and Fatigue in Structural Materials – From Macro to Nano: Proceedings of the Hael Mughrabi Honorary Symposium, edited by K. Jimmy Hsia et al., TMS (2008), p. 229.

[7] N. Thompson, N. Wadsworth and N. Louat, Phil. Mag. 1 (1956) 113.

[8] R. Zauter, F. Petry, M. Bayerlein, C. Sommer, H.-J. Christ and H. Mughrabi, Phil. Mag. A 66 (1992) 425.

[9] H. Mughrabi and R. Wang, in: Deformation of Polycrystals: Mechanisms and Microstructures, Proceedings of 2nd Risø International Symposium on Metallurgy and Materials Science, edited by N. Hansen et al., Roskilde: Risø National Laboratory (1981) p. 87.

[10] K. Differt, U. Essmann and H. Mughrabi, Phil. Mag. A 34 (1986) 237.

[11] R. Wang and H. Mughrabi, Mat. Sci. Eng. 63 (1984) 16.

[12] T.G. Langdon and R.C. Gifkins, Scripta metall. 13 (1979) 1191.

[13] V. Raman and T.G. Langdon, J. Mater. Sci Letters 2 (1983) 180.

[14] S. Weiss and G. Gottstein, Mater. Sci. and Technol. 14 (1998) 1169.